# Superparamagnetism and magnetic properties of Ni nanoparticles embedded in SiO₂

F. C. Fonseca, G. F. Goya, and R. F. Jardim*

*Instituto de Física, Universidade de São Paulo, CP 66318, 05315-970, São Paulo, SP, Brazil*

R. Muccillo

*Centro Multidisciplinar de Desenvolvimento de Materiais Cerâmicos CMDMC, CCTM-Instituto de Pesquisas Energéticas e Nucleares, CP 11049, 05422-970, São Paulo, SP, Brazil*

N. L. V. Carreño, E. Longo, and E. R. Leite

*Centro Multidisciplinar de Desenvolvimento de Materiais Cerâmicos CMDMC, Departamento de Química, Universidade Federal de São Carlos, CP 676, 13560-905, São Carlos, SP, Brazil*

We have performed a detailed characterization of the magnetic properties of Ni nanoparticles embedded in a SiO₂ amorphous matrix. A modified sol-gel method was employed which resulted in Ni particles with average radius $\sim 3$ nm, as inferred by TEM analysis. Above the blocking temperature $T_B \approx 20$ K for the most diluted sample, magnetization data show the expected scaling of the $M/M_S$ vs $H/T$ curves for superparamagnetic particles. The hysteresis loops were found to be symmetric about zero field axis with no shift via exchange bias, suggesting that Ni particles are free from an oxide layer. For $T < T_B$ the magnetic behavior of these Ni nanoparticles is in excellent agreement with the predictions of randomly oriented and noninteracting magnetic particles, as suggested by the temperature dependence of the coercivity field that obeys the relation $H_C(T) = H_{C0}[1 - (T/T_B)^{1/2}]$ below $T_B$ with $H_{C0} \sim 780$ Oe. The obtained values of $H_{C0}$, considering the temperature dependence of the magnetic anisotropy constant, are discussed within the scenario of isolated randomly oriented and noninteracting single-domain particles.

PACS number(s): 75.50.Tt, 75.50.Kj, 75.25.+z

## I. INTRODUCTION

Nanosized particles of ferromagnetic metals such as Fe, Co, and Ni are the focus of growing interest because of both the richness of their physical properties and potential applications like catalysts, high density magnetic recording media, ferrofluids, and medical diagnostics.[1–4] In 1946 Kittel[5] clearly established, by energy considerations, that a single magnetic domain would be more stable for particles below a certain critical size (e.g., $\approx 10^{-8}$ m for iron), and Néel[6] pointed out that for such small particles thermal agitation will prevent the existence of stable magnetization, leading to a superparamagnetic (SPM) state. The pioneering work of Stoner and Wohlfarth (SW) provided a model of magnetization reversal in single-domain particles,[7] consisting of a coherent rotation of the magnetic moments. The experimental difficulties in manufacturing nanoparticle systems of good quality hindered a precise comparison to the SW model until recent years, when delicate works on isolated nanoparticles of Co,[8–10] Fe,[11] Ni nanoparticles dispersed in silica,[12] and Co nanoclusters[13] showed that although the SW model accurately describes the magnetic behavior, it fails to account for more subtle microscopic mechanisms, as discussed in Ref. 14. But, as the magnetization reversal in the frozen state will depend on the dominant magnetic anisotropy, very different magnetic properties should be expected for fine particles with high and low crystal anisotropies, provided that shape or stress anisotropies are not predominant. Although comparative studies on Ni and Co nanowires have revealed that the different crystalline anisotropies of both materials yield different magnetic behaviors,[15] studies on low anisotropy

single-domain particles are lacking. Ultrafine Ni particles provide a good example of such low coercivity materials.

Isolated Ni nanoparticles can be obtained by evaporation,[16] and other techniques like sputtering,[17] high-energy ball milling,[12] ion exchange,[18] and sol-gel[19,20] have been used to embed Ni particles in an inert, nonmagnetic matrix. Particularly, preparation of Ni nanoparticles dispersed in porous matrix, typically silica, exhibit two main problems: the control of the size of the particles, and the oxidation of the particle surface. The control of the average size of the particles strongly depends on the parameters of the preparation method. However, because of the very high surface area to volume ratio, these particles have a high reactivity and can be easily environmentally degraded. This usually results in particles with a shell-core morphology where an antiferromagnetic (AFM) oxide layer surrounds the ferromagnetic particles, which can yield misleading conclusions from the magnetic data.

In this work, we present a detailed study on the magnetic properties of high-quality Ni nanoparticles of about 3 nm with very narrow particle size distribution, oxide free, prepared through a modified sol-gel precursor method.[20] We found that the magnetic properties of such particles are precisely described by a model of thermally activated, randomly oriented and noninteracting SPM particles, by taking into account the temperature dependence of the magnetic anisotropy. We also show that interparticle interactions are readily observable for highly diluted samples, indicating that the ordinary criteria for defining a magnetically diluted system of noninteracting particles must be revised.

## II. EXPERIMENT

Nanocomposites of Ni:SiO$_2$ were synthesized by using tetraethylorthosilicate (TEOS), citric acid, and nickel (II) nitrate. The citric acid was dissolved in ethanol and the TEOS and nickel nitrate were added together and mixed for homogenization at room temperature. The polymerizing reaction was promoted by adding ethylene glycol to the citrate solutions at temperatures close to 100 °C. The solid resin was heated at 300 °C for 6 h, ground in a ball mill, and then pyrolyzed at 500 °C. Further details of the method employed can be found elsewhere.[20] Here we concentrate our discussion in two diluted samples with ~1.5- and 5-wt. % Ni which are referred in the text as samples $S1$ and $S2$, respectively.

The structure and morphology of the magnetic powders were examined by transmission electron microscopy TEM with a Philips CM200, 200-kV, high-resolution transmission microscope. Observations of the nanocomposites were performed on a drop of powder suspension deposited on an amorphous carbon-coated nickel grid.

Magnetization measurements $M(T,H)$ in applied magnetic fields between ±7 T and for temperatures ranging from 2 to 300 K, were performed in powders conditioned in gelatin capsules with a Quantum Design SQUID (superconducting quantum interference device) magnetometer. To determine the coercivity field few steps were followed: (a) first, the sample was cooled in zero applied magnetic field from room temperature down to the measuring temperature; (b) second, hysterisis loops were measured in magnetic fields ranging from ±7 T. Between each hysteresis loop the sample was warmed up to room temperature, and the steps described above were repeated.

## III. RESULTS AND DISCUSSION

Figure 1 shows a low magnification TEM bright field (BF) image of the $S1$ sample. It is observed that the Ni nanoparticles (dark spots in the photograph) are well dispersed in the amorphous SiO$_2$ matrix. BF-TEM analysis revealed that the Ni particles present an homogeneous particle size distribution, with a mean particle size of ~3.3 nm (see the high magnification BF-TEM image in the inset of Fig. 1).

The temperature dependence of the magnetization $M(T)$ of both samples, taken in zero-field-cooling (ZFC) and field-cooling (FC) conditions (Fig. 2), exhibits the main features of SPM systems: (1) the ZFC curves are rounded at the blocking temperature $T_B$, defined as the temperature of the maximum, indicating a blocking process of the small particles; and (2) a paramagneticlike behavior above $T_B$. It is important to notice that above $T_B$, the $\chi^{-1}$ (not shown) is roughly linear with temperature in agreement with the Curie law. At high temperatures, roughly ~220 K, where the magnetic susceptibility of the system is very small, this linearity breaks down. This, as observed in nanoparticles of Co (Ref. 9) and Ni (Ref. 21), is due to a temperature-dependent saturation magnetization which decreases the particle's superparamagnetic moment, increasing the slope of $\chi^{-1}$ versus $T$ at high temperatures. The data also indicate that $T_B$ shifts
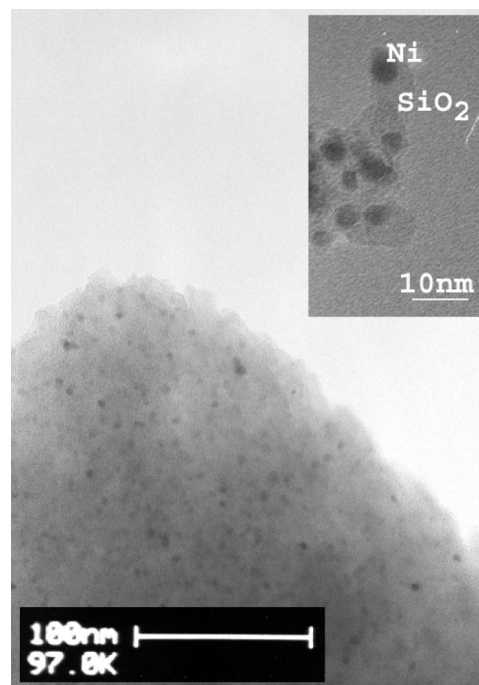


FIG. 1. Transmission electron micrograph of Ni nanoparticles embedded in an amorphous SiO$_2$ matrix.

from $T_B \sim 20$ K for the $S1$ sample to $T_B \sim 40$ K for the more concentrated $S2$ sample, in agreement with either a larger average size particle and Ni concentration of sample $S2$.[21]

The SPM behavior of these samples above $T_B$ was confirmed by magnetic hysteresis loops measured between 2 and 200 K, as shown in Fig. 3 for the more diluted sample $S1$. Let us concentrate first on the curves taken in the high temperature regime. The $M/M_S$ curves plotted against $H/T$ for $T > T_B$ results in a universal curve. This scaling is consistent with SPM response, though it is strictly only a true scaling at low fields for temperatures above $T_B$. In addition, above $T_B$, the contribution from the SPM particles to the total magne-
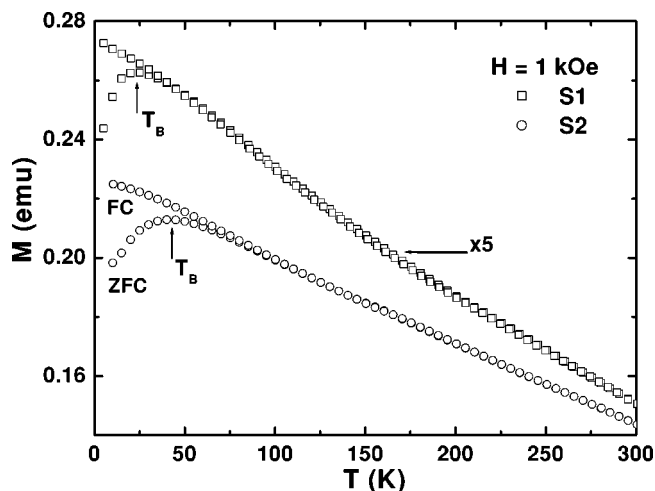


FIG. 2. Temperature dependence of the magnetization for samples $S1$ and $S2$. Curves were taken in the ZFC and FC processes at $H = 1$ kOe.
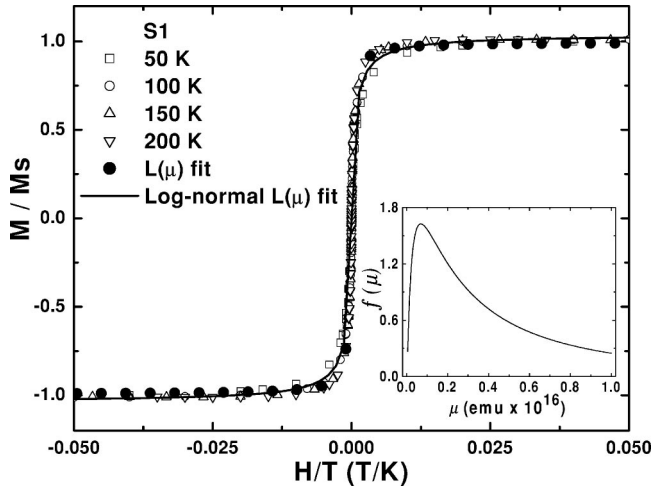
FIG. 3. Normalized magnetization as a function of $H/T$ at temperatures of 50, 100, 150, and 200 K for nanocrystalline Ni particles. The inset shows the log-normal distribution $f(\mu)$ of the magnetic moments, as described in the text.

tization is described by $M=M_S L(x)$, where $M_S=N\mu$ is the saturation magnetization due to N particles with magnetic moment $\mu$, and $L(x)$ is the Langevin function with $x=\mu H/k_B T$. This expression assumes that the system is comprised of *noninteracting* and *monodisperse* particles. However, since real systems do have a distribution of magnetic moments, the magnetization of SPM grains in a magnetic field $H$ is better described as a weighted sum of Langevin functions[22,23]

$$M=\int_0^\infty L\left(\frac{\mu H}{k_B T}\right)f(\mu)d\mu, \tag{1}$$

where $f(\mu)$ is the distribution function of magnetic moments related to the saturation magnetization by

$$M_S=\int_0^\infty f(\mu)d\mu. \tag{2}$$

Equations (1) and (2) assume that $M_S$ is nearly temperature-independent, a condition valid provided that $T_B \ll T \ll T_C$. Therefore, our analysis has been restricted to the $50 < T < 200$ K range, since $T_B < 40$ K and $T_C \sim 650$ K. To perform the calculations we have used a log-normal distribution of $\mu$ values,

$$f(\mu)=\frac{1}{\sqrt{2\pi}\mu\sigma}\exp\left(-\frac{\ln^2(\mu/\mu_0)}{2\sigma^2}\right), \tag{3}$$

where $\sigma$ is the distribution width and $\mu_0$ is the median of the distribution related to the average (mean) magnetic moment $(\mu_m)$ by $\mu_m=\mu_0\exp(-\sigma^2/2)$. Table I shows the best-fit parameters obtained for samples $S1$ and $S2$, using Eqs. (1) and (2), and a single Langevin function. Although both fits lead to comparable results, the most important difference arises from the magnetic moment values. The simple Langevin fitting results in a magnetic moment $\mu$ close to the median value $\mu_0$ obtained from the log-normal weighted fitting but

TABLE I. Best-fit parameters for $M/M_S(H,T)$ vs $H/T$ curves and calculated radii of spherical particles. Magnetic moment values in emu$\times 10^{17}$ and radii in nm.

| Sample | weighted $L(x)$ | | | | | simple $L(x)$ | | |
|---|---|---|---|---|---|---|---|---|
| | $\mu_0$ | $\mathbf{r}_0$ | $\mu_m$ | $\mathbf{r}_m$ | $\sigma$ | $\mu$ | $\mathbf{r}$ | $\mathbf{r}_{T_B}$ |
| $S1$ | 4.6 | 2.8 | 12 | 3.8 | 1.4 | 5.2 | 2.9 | 2.5 |
| $S2$ | 5.1 | 2.9 | 17 | 4.4 | 1.6 | 6.1 | 3.1 | 3.1 |

the mean magnetic moment $\mu_m$ obtained by the latter is higher. The radii of supposed spherical particles calculated from the respective magnetic moment values are in excellent agreement with TEM observations (Table I).

Turning now to the low temperature regime, Fig. 4 shows the hysteresis loops measured at temperatures ranging from 3.5 to 50 K. We remark that NiO/Ni composites exhibit an exchange bias due to interfacial interaction between ferromagnetic Ni and AFM NiO.[24] This exchange interaction is evidenced through a shift of hysteresis loops along the field axis when the system is field-cooled below the ordering temperature of the AFM phase. Defining $H_{C^+}$ and $H_{C^-}$ as the coercive fields with decreasing and increasing fields, respectively, a measure of the symmetry of the $M(H)$ curves is given by $\Delta H_C=(H_{C^+}+H_{C^-})/2$. Previous works on Ni/NiO systems reported values for the exchange bias field $\Delta H_C$ ranging from $\approx 80$ Oe in Ni/NiO nanowires,[25] to $\sim 700$ Oe in partially oxidized Ni nanoparticles.[26] The hysteresis loops displayed in Fig. 4 clearly show that these loops are symmetric about zero field ($\Delta H_C \sim 1$ Oe) indicating the absence of particles with the shell-core NiO-Ni morphology. The data also indicate a negligible contribution of isolated NiO nanoparticles, which would exhibit large loop shifts of up to $\sim 10$ kOe.[27] Thus our magnetic data strongly suggest that the modified sol-gel method used for the synthesis of nanosized Ni metallic particles results in significantly less oxidized metallic particles than other techniques.[25,26]
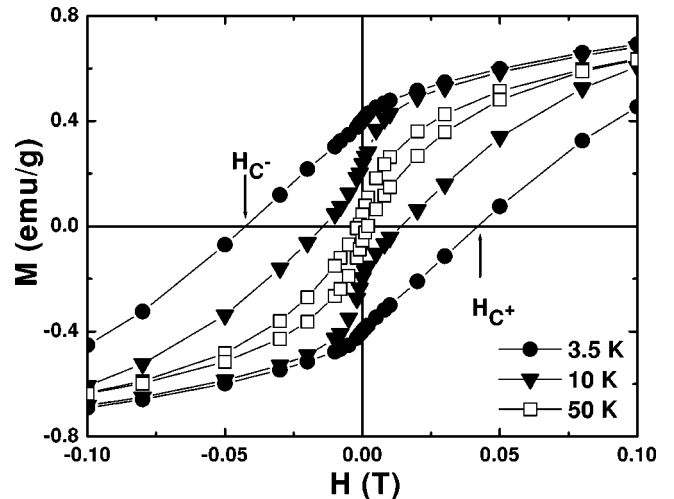


FIG. 4. Expanded view of hysteresis loops taken at 3.5, 10, and 50 K for nanocrystalline Ni particles. $H_{C^+}$ and $H_{C^-}$ are defined in the text.
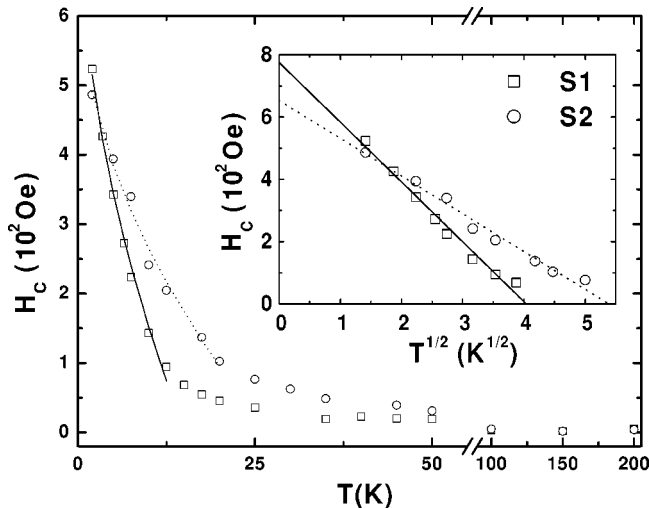
FIG. 5. Temperature dependence of the coercivity $H_C$ for samples $S1$ and $S2$. The inset shows $H_C(T)$ to obey a $(T)^{1/2}$ dependence with $H_{C0}$ of $\sim 780$ and 650 Oe for samples $S1$ and $S2$, respectively.

The $H_C(T)$ values at different temperatures (Fig. 5) reveal that coercivity develops appreciably below $T_B \sim 20$ and 40 K for samples $S1$ and $S2$, respectively, in agreement with blocking temperatures inferred from $M(T)$ curves. The coercivity for a system of *randomly oriented and noninteracting particles* is expected to follow the relation

$$H_C(T) = H_{C0}\left[1 - \left(\frac{T}{T_B}\right)^{1/2}\right],\qquad (4)$$

with $H_{C0} = 0.64K/M_S$,[28] where $K$ is the anisotropy constant of bulk Ni, $M_S$ is the saturation magnetization, and $T_B = K\langle V\rangle/25k_B$. The above expression considers that the magnetization reversal takes place coherently, a situation that can be achieved *when interparticle interactions are neglected*.[7,29,30] Figure 5 shows that this dependence is closely followed by both samples, supporting the picture of noninteracting particles, as previously observed in systems comprised of metallic and ferromagnetic nanoparticles.[8,11,31] Also, the extrapolation of $H_C(T)$ to 0 yields values of $T_B \sim 16$ and $\sim 27$ K for samples $S1$ and $S2$, respectively, consistent with those obtained from $M(T)$ curves.

From these $T_B$ values, Eq. (4) also gives an estimation of the radius $r_{T_B}$ of the assumed spherical particle. We note here that the first-order magnetocrystalline anisotropy $K_1$ of bulk Ni displays a large increase with decreasing temperature given by $K_1(T) = K_0\exp(-aT^2)$, where $K_0 = -8 \times 10^5$ erg/cm³ and $a = 3.4 \times 10^{-5}$.[32] Since $K_1(T)$ is nearly temperature independent below 50 K, we have used the zero-temperature extrapolated value of $K_1 \sim -8 \times 10^5$ erg/cm³ for fcc Ni to estimate $r_{T_B}$ of $\sim 2.5$ and 3.1 nm for samples $S1$ and $S2$, respectively. These values are in excellent agree-

ment with those obtained from TEM and $M(H)$ data, as shown in Table I.

Equation (4) also gives additional information regarding $H_C$ at low temperatures. By using the appropriate expression $H_{C0} = 0.64K_1/M_S$ for randomly oriented and noninteracting particles and the Ni bulk value $M_S (T=0) = 541$ emu/cm³, we found $H_{C0} \sim 950$ Oe. This zero-temperature coercivity field is similar to the one of $\sim 780$ Oe obtained for sample $S1$ by the extrapolation of the $H_C$ vs $T^{1/2}$ curve, as shown in the inset of Fig. 5. These results indicate that the model for randomly and noninteracting particles gives appropriate values for the coercivity at low temperatures, at least for the more diluted sample $S1$. The difference of $\sim 20\%$ between the predicted and the *lower* experimental coercivities extrapolated to $T=0$ may be associated to incoherent magnetization reversal processes, such as fanning and curling, related to weak magnetic interactions which are expected to decrease $H_{C0}$. These mechanisms are known to be determinant in patterned materials, as previously observed in nanometric Ni chains and wires[33,34] where incoherent rotation by curling can reduce the reversing field down to $\sim 30\%$ of the calculated for rotation in unison. Although TEM micrographs of our samples do not show evidence of significant particle agglomeration, dipolar interactions that might induce an evolution of the magnetization reversal toward more incoherent and heterogeneous mechanisms cannot be ruled out.

## IV. CONCLUSION

In summary, we have prepared Ni nanoparticles embedded in SiO₂ amorphous matrix which exhibit superparamagnetism above $T_B < 40$ K. The magnetic characterization of these materials indicates that metallic particles are free from an oxide layer, as inferred from the absence of exchange bias in hysteresis loops taken at temperatures below $T_B$. The magnetic behavior of the more diluted samples is consistent with the predictions of systems having randomly oriented and noninteracting small particles when the temperature dependence of the magnetic anisotropy is considered. The small difference between predicted and observed coercivity fields at zero temperature $H_{C0}$ is still an open problem.

*Electronic address: rjardim@if.usp.br

[1] L. Schultz, K. Schitzke, and J. Wecker, Appl. Phys. Lett. **56**, 868 (1990).

[2] L. Lu, M. L. Sui, and K. Lu, Science **287**, 1463 (2000).

[3] M. Ozaki, Mater. Res. Bull. **XIV**, 35 (1989).

[4] H. Gleiter, Nanostruct. Mater. **1**, 1 (1992).

[5] C. Kittel, Phys. Rev. **70**, 965 (1946).

[6] L. Néel, Ann. Geophys. (C.N.R.S.) **5**, 99 (1949).

[7] E. C. Stoner and E. P. Wohlfarth, Philos. Trans. R. Soc. London, Ser. A **240**, 599 (1948).

[8] M. E. McHenry, S. A. Majetich, J. O. Artman M. DeGraef, and S. W. Staley, Phys. Rev. B **49**, 11 358 (1994).

[9] J. P. Chen, C. M. Sorensen, K. J. Klabunde, and G. C. Hadjipanayis, Phys. Rev. B **51**, 11 527 (1995).

[10] E. Bonet, W. Wernsdorfer, B. Barbara, A. Benoit, D. Mailly, and A. Thiaville, Phys. Rev. Lett. **83**, 4188 (1999).

[11] S. Linderoth, L. Balcells, A. Labarta, J. Tejada, P. V. Hendriksen, and S. A. Sethi, J. Magn. Magn. Mater. **124**, 269 (1993).

[12] E. M. González, M. I. Montero, F. Cebollada, C. de Julián, J. L. Vicent, and J. M. González, Europhys. Lett. **42**, 91 (1998).

[13] M. Jamet, W. Wernsdorfer, C. Thirion, D. Mailly, V. Dupuis, P. Mélinon, and A. Pérez, Phys. Rev. Lett. **86**, 4676 (2001).

[14] A. Thiaville, Phys. Rev. B **61**, 12 221 (2000).

[15] R. Ferré, K. Ounadjela, J. M. George, L. Piraux, and S. Dubois, Phys. Rev. B **56**, 14 066 (1997).

[16] T. Hayashi, T. Ohno, S. Yatsuya, and R. Ueda, Jpn. J. Appl. Phys. **16**, 705 (1977).

[17] A. Gavrin and C. L. Chen, J. Appl. Phys. **73**, 6949 (1993).

[18] J. S. Jung, W. S. Chae, R. A. McIntyre, C. T. Seip, J. B. Wiley, and C. J. O'Connor, Mater. Res. Bull. **34**, 1353 (1999).

[19] C. Estournès, T. Lutz, J. Happich, T. Quaranta, P. Wissler, and J. L. Guille, J. Magn. Magn. Mater. **173**, 83 (1997).

[20] E. R. Leite, N. L. V. Carreño, E. Longo, A. Valentini, and L. F. D. Probst, J. Nanosci. Nanotechnol. **2**, 89 (2002).

[21] J. Gittleman, B. Abeles, and S. Bozowski, Phys. Rev. B **9**, 3891 (1974).

[22] E. F. Ferrari, F. C. S. da Silva, and M. Knobel, Phys. Rev. B **56**, 6086 (1997).

[23] J. C. Cezar, M. Knobel, and H. C. N. Tolentino, J. Magn. Magn. Mater. **226-230**, 1519 (2001).

[24] J. B. D. Cullity, *Introduction to Magnetic Materials* (Addison-Wesley, Reading, MA, 1972), Chap. 11.

[25] M. Fraune, U. Rudiger, G. Guntherodt, S. Cardoso, and P. Freitas, Appl. Phys. Lett. **77**, 3815 (2001).

[26] Y. D. Yao, Y. Y. Chen, M. F. Tai, D. H. Wang, and H. M. Lin, Mater. Sci. Eng., A **217**, 837 (1996).

[27] R. H. Kodama, S. A. Makhlouf, and A. E. Berkowitz, Phys. Rev. Lett. **79**, 1393 (1997).

[28] R. M. Bozorth, *Ferromagnetism* (Van Nostrand, Princeton, NJ, 1956), Chap. 18, p. 831.

[29] E. F. Kneller and F. E. Luborsky, J. Appl. Phys. **34**, 656 (1963).

[30] D. Kechrakos and K. N. Trohidou, Phys. Rev. B **58**, 12 169 (1998).

[31] X. C. Sun, X. L. Dong, and J. A. Toledo, J. Nanosci. Nanotechnol. **1**, 291 (2001).

[32] H. J. Williams and R. M. Bozorth, Phys. Rev. **56**, 837 (1939).

[33] P. M. Paulus, F. Luis, M. Kröll, G. Schmid, and L. J. de Jongh, J. Magn. Magn. Mater. **224**, 2 (2001).

[34] J. I. Martín, J. L. Costa-Kramer, F. Briones, and J. L. Vicent, J. Magn. Magn. Mater. **221**, 215 (2000).